Current Applied Physics 14 (2014) 1788–1793

Contents lists available at ScienceDirect

Current Applied Physics

journal homepage: www.elsevier.com/locate/cap

Thermoelectric generator based on a bismuth-telluride alloy fabricated by addition of ethylene glycol

Kyung Kuk Jung, Jong Soo Ko*

Graduate School of Mechanical Engineering, Pusan National University, Busandaehak-ro 63beon-gil, Geumjeong-gu, Busan 609-735, Republic of Korea

ARTICLE INFO

Article history:
Received 2 June 2014
Received in revised form
17 September 2014
Accepted 7 October 2014
Available online 17 October 2014

Keywords:
Thermoelectric generator
Bismuth telluride alloy
Pulse electrodeposition
Ethylene glycol

ABSTRACT

This paper introduces a new method to selectively fabricate n-type and p-type bismuth (Bi)-telluride (Te) thermoelectric materials by the rate of addition of ethylene glycol (EG) in the Bi–Te co-electrodeposition solution. As the amount of added EG is increased, the atomic ratio of Bi in the deposited Bi–Te alloy reached a slope of 0.463 (at.% of Bi/vol.% of EG), and increased in a linear manner. When the EG content reached approximately 20%v/v, the n-type material changed into a p-type. This change implies that adjusting the EG content in the electrodeposition solution affords simple control of the Bi–Te composition. To demonstrate the applicability of the developed thermoelectric materials, thermoelectric generators (TEGs) were fabricated using electrodeposited n-type (using solution without EG) and p-type (using solution with 30%v/v EG) Bi–Te alloys. The Seebeck voltage of the pair of n-type and p-type thermoelectric materials was 140 mV and the power generated from the pair was 24.36 nW at a 10 °C temperature difference.

1. Introduction

A thermoelectric generator (TEG) is an energy conversion device that directly converts heat energy into electrical energy. When a heat source exists it is able to produce electricity without other mechanical actuating elements. Continuous generation of electricity is therefore possible and the device has the advantage of not causing vibration or noise. Recently, the development of thermoelectric elements using body heat has been actively pursued and such technology has been commercialized in the form of wristwatches, which consume relatively little energy [1]. Wearable thermoelectric devices are limited by the area of the device. Improvement of the thermoelectric material performance index, along with miniaturization and high integration of the thermocouple, which is composed of a pair of p-type and n-type thermoelectric materials, are therefore necessary in order to increase electricity production.

For the development of thermoelectric materials and high integration of such materials, various methods that are used in nano- and micromachining technologies have recently been actively utilized to fabricate TEGs. Evaporation [2], sputtering [3], metal organic chemical vapor deposition (MOCVD) [4], and electrodeposition [5] are the main approaches used for the deposition of thermoelectric materials. Among these methods, electrodeposition is relatively inexpensive and provides high deposition speeds. It also offers the advantage of a capability to form large area films. Moreover, electrodeposition can be selectively applied and the p-type and n-type thermoelectric materials can be formed at desired locations [6].

Research on Bismuth (Bi)-Telluride (Te) alloy deposition using electrodeposition has recently increased [5,7–9]. When the Bi atomic percent (at.%) in the coated Bi–Te alloy is lower than 40%, the material becomes n-type, whereas it becomes p-type above this level [6]. In order to fabricate two different types of thermoelectric materials, various methods to control the applied current, voltage, temperature of the electrolyte, stirring speed of the solution, and Bi–Te content have been developed [6,8,10]. However, obtaining thermoelectric materials with the desired Bi–Te composition ratio by controlling the above variables is very complicated and a significant amount of time and effort are required to establish suitable processing conditions.

This study presents a new method to control the Bi and Te composition ratio in the deposited alloy film by controlling only the ethylene glycol (EG) content in the Bi–Te co-electrodeposition solution. TEGs are then fabricated using the p-type and n-type Bi–Te thermoelectric materials developed in this study to demonstrate

* Corresponding author.
E-mail address: mems@pusan.ac.kr (J.S. Ko).

http://dx.doi.org/10.1016/j.cap.2014.10.010
1567-1739/

their possible applicability and their performance is evaluated. P-type and n-type thermoelectric columns are embedded in a polymer (SU-8) substrate and they are electrically connected in series.

2. Experimental

2.1. Preparation of Bi–Te thermoelectric films

To fabricate the electrodeposition solution, the volume ratio of ethylene glycol (107-21-1, Alfa Aesar, USA, 99%) was varied (0, 10, 20, 30, 40%v/v) in the solutions composed of 10 mM Bi (LEES CHEM, Korea, 99.9%), 10 mM TeO_2 (Alfa Aesar, UK, 99.99%), and 1 M HNO_3 (70% electronic grade, OCI Company, Korea). The mole concentrations of Bi, TeO_2, and HNO_3 were maintained in all electrodeposition solutions, regardless of the EG content. For the solutions, deionized water (OCI Company, Korea) with a specific resistance over 18 MW•cm was used throughout the study. A potentiostat (Versastat2, Princeton Applied Research, USA) was used for the electrodeposition. A 2.5 × 2.5 cm^2 platinum mesh (i-Nexus, USA) was used as the counter electrode and Ag/AgCl/KCl +0.197 V vs SHE (Princeton Applied Research, USA) was used as the reference electrode. A scanning electron microscopy (SEM) (S-4800, HITACHI, Japan), energy dispersive spectroscopy (EDS) (7593-H, HORIBA, Japan) and X-ray diffraction (XRD) system (D8 advance, Bruker, USA) were used to analyze the formed structure's shape, composition and lattice structure.

After forming a silicon dioxide film of 300 nm thickness on the silicon wafer, Ti (10 nm)/Au (300 nm) was sequentially deposited via sputtering (ENDURA-5500, AMAT, USA). While the silicon dioxide served as an insulation layer, the Ti/Au layer played the role of a conducting seed layer for electrodeposition. The electrodeposition area was fixed at 10 × 10 mm^2, and the gaps between the working electrode, reference electrode, and counter electrode were maintained at 10 mm. The applied current during electrodeposition was −100 mA/cm^2 and of a pulse wave form. One cycle was composed of pulse on-time (0.1 s) and off-time (5 s), and electrodeposition was performed for a total of 3,000 cycles for each specimen. The temperature of the electrodeposition solution was 18 °C and electrodeposition was done with no stirring.

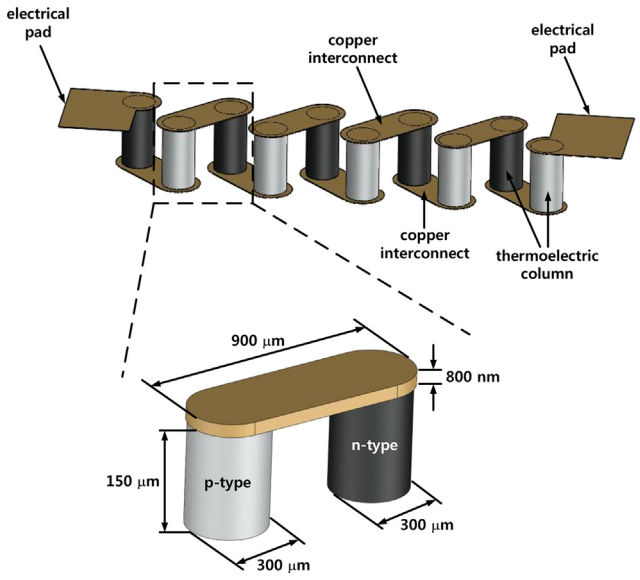

Fig. 1. Configuration of a TEG having five thermocouples. The SU-8 substrate is not shown in the figure for better visualization of the core components.

2.2. Design and fabrication of TEG

Fig. 1 shows the design of the proposed TEG, wherein five thermocouples are connected in series. Each thermocouple is composed of a pair of p-type and n-type thermoelectric columns. The open circuit Seebeck voltage generated by a TEG can be expressed as [11]

$$V_o = n\alpha_{pn}\Delta T_{TEG} \quad (1)$$

where n is the number of thermocouples, α_{pn} the relative Seebeck coefficient of the p-type and n-type thermoelectric materials, and ΔT_{TEG} the temperature difference between the cold and hot surfaces of the TEG. Power is the product of the output voltage and electrical current. Therefore, the maximum output power generated by a TEG can be expressed as

$$P_o = \left(n\alpha_{pn}\Delta T_{TEG}\right)^2 \Big/ 4R_{TEG} \quad (2)$$

where R_{TEG} denotes the internal electrical resistance.

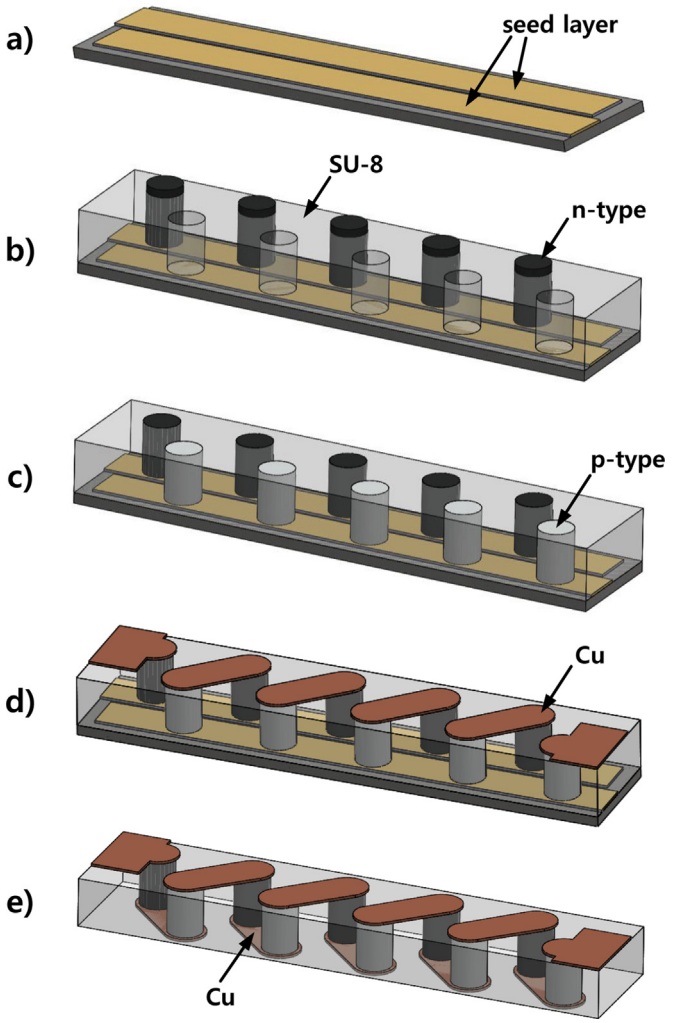

Fig. 2. Microfabrication process sequence of TEGs: (a) Ti/Au conducting seed layer deposition and patterning, (b) photolithography using SU-8 and electrodeposition of n-type thermoelectric material, (c) electrodeposition of p-type thermoelectric material and CMP of the top surface, (d) topside Cu deposition, and (e) removal of Si substrate and Ti/Au seed layer by CMP process and bottom side Cu deposition.

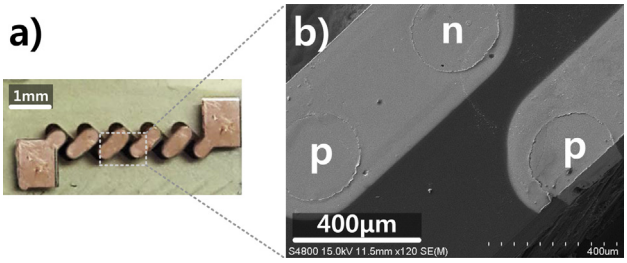

Fig. 3. (a) A photo of a fabricated TEG where five thermocouples are connected in series and (b) a cross-sectional SEM image of a thermocouple.

The two different type thermoelectric columns were designed to be the same size: 300 μm in diameter and 150 μm in height. The designed length of a pair of p-type and n-type thermocouples was 900 μm and the thickness of the copper interconnect was 800 nm.

Fig. 2 shows schematic illustrations of the process sequence to fabricate a TEG. First, a Ti (10 nm)/Au (300 nm) conducting seed layer was deposited on a 6-inch Si wafer (LG Siltron, Korea) followed by photolithography using AZ-1512 (AZ Electronic Materials, UK), and then the exposed Ti/Au layer was etched (Fig. 2a). Second, photolithography was carried out using SU-8 2050 (MICROCHEM, USA), followed by the first Bi–Te alloy electrodeposition using a Bi–Te electrodeposition solution without ethylene glycol to form n-type thermoelectric columns (Fig. 2b). A 180 μm-thick photoresist was fabricated and 187 μm-high n-type Bi–Te columns were obtained with the current conditions noted in Section 2.1 for 25,000 cycles. Third, the second Bi–Te alloy electrodeposition using a Bi–Te electrodeposition solution mixed with 30%v/v ethylene glycol was carried out to form p-type thermoelectric columns (Fig. 2c). 173 μm-high p-type Bi–Te columns were obtained with the current conditions noted in Section 2.1 for 25,000 cycles. Fourth, the surface of the electrodepositied Bi–Te and SU-8 layer photoresist was flattened by a chemical mechanical polishing (CMP) process. Then, to form topside Cu interconnects, an 800 nm-thick Cu layer was deposited on the topside of the processing substrate using a thermal evaporator (ULTECH, Korea) (Fig. 2d). By using a nickel shadow mask, Cu was deposited on only the selected topside area, as shown in Fig. 2d. Finally, the Si substrate and Ti/Au layer were sequentially removed by a second CMP process. The thickness of the electrodeposited Bi–Te and SU-8 photoresist layer was adjusted to 150 μm through the CMP process. Then, to form bottom side Cu interconnects, an 800 nm-thick Cu layer was deposited on the bottom side of the processing substrate (Fig. 2e). For the selective deposition of Cu, another nickel shadow mask was used and Cu was deposited only on the selected bottom side area, as shown in Fig. 2e. Fig. 3a, b shows a photo of a fabricated TEG that has five thermocouples and a cross-sectional SEM image of a pair of fabricated n-type and p-type thermoelectric columns, respectively.

2.3. Measurement scheme

To obtain the Seebeck coefficient of the fabricated thermoelectric films, as shown in Fig. 4a, a temperature difference was applied by attaching Peltier plates (FALC1-03150T125, Ntrex, Korea) on the left and right sides of the fabricated films. Here, the produced voltage was measured. Two Peltier plates of 30 × 30 mm^2 were situated side by side with a distance (d) of 8 mm. The sizes of the electrodeposited films were 10 × 10 mm^2. When a film was placed at the center of the two Peltiers, a 1 mm wide portion of the left side of the film was placed on the cold Peltier plate (18 °C), while a 1 mm wide portion of the left side was placed on the hot Peltier plate (28 °C). To minimize the thermal contact resistance between the thermoelectric films and the Peltier plates, thermal grease (ZM-TG2, Zalman, Korea) was used. An electrode was created using silver paste (CPT-100, CANS, China) on each side of the films. A surface temperature measurement sensor (STS-BTA, Vernier, USA) was used to measure the temperature of the Peltier surface. The produced voltage was measured using a precision multimeter (USB-4065, National Instruments, USA). Fig. 4b shows the measurement scheme for the performance evaluation of the fabricated TEGs. A hot Peltier plate (28 °C), a fabricated device, and a cold Peltier plate (18 °C) are sequentially stacked from the top to apply uniform temperatures to the upper and lower surfaces of the device. Thermal grease was also used for this measurement.

3. Results and discussion

3.1. Bi–Te thermoelectric films

The XRD pattern in Fig. 5 indicates that the electrodeposited material has a single rhombohedral lattice structure of Bi_2Te_3 (space group of R3 m). It is observed that the films deposited at EG 0 and 10% have a preferred orientation of the (015) lattice plane. Above EG 10%, however, the peak positions and their intensities were obviously changed to the (104) lattice plane. The peaks can be indexed through comparison with a powder diffraction file based on JCPDS card No. 15-863. Fig. 6a–e shows SEM images of the deposited Bi–Te using solutions with 0, 10, 20, 30, and 40%v/v added EG. As the EG content was increased, the coated Bi/Te particle size showed a declining trend (0%v/v: 92 ± 5 nm, 10%v/v: 76 ± 6 nm, 20%v/v: 48 ± 6 nm, 30%v/v: 32 ± 3 nm, 40%v/v: 21 ± 3 nm). This was due to the relatively high overpotential in the pulse electrodeposition conditions compared to the electrodeposition in the conventional constant voltage and current conditions [12]. The following reactions occur in the cathode during Bi–Te electrodeposition [13,14]:

$$TeO_2(s) + 4H^+ + 4e^- \rightarrow Te(s) + 2H_2O \quad (3)$$

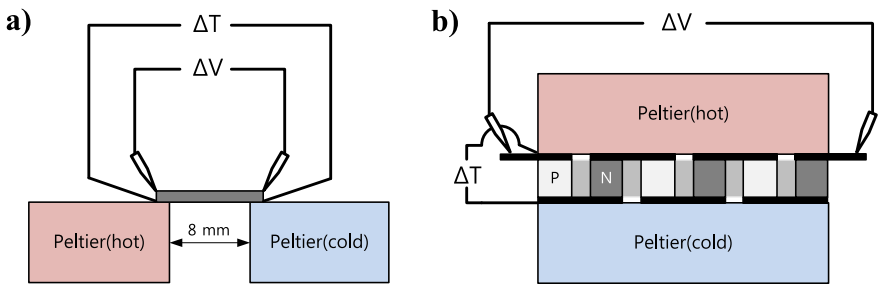

Fig. 4. (a) Measurement scheme for the Seebeck coefficients of the electrodeposited Bi–Te films (tilted view) and (b) measurement scheme for the output voltages of the fabricated TEGs (side view).

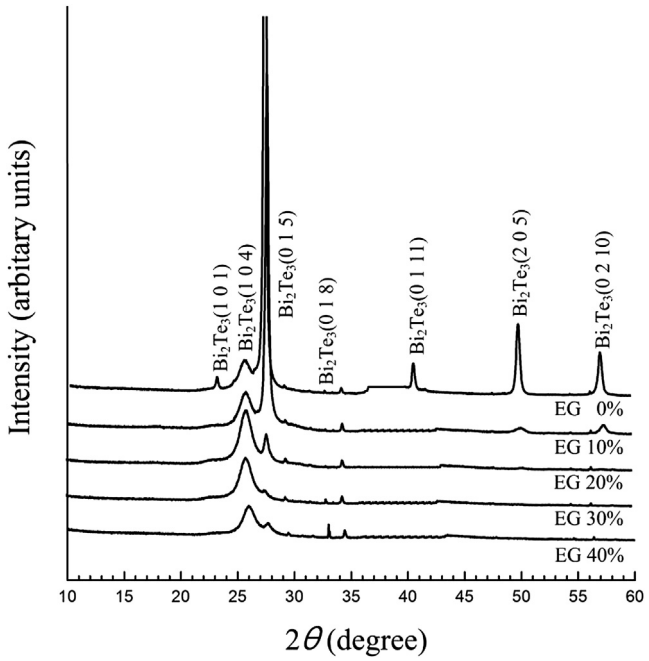

Fig. 5. X-ray diffraction patterns of bismuth telluride films deposited at various concentrations of ethylene glycol.

$$Bi^{3+} + 3e^{-} \rightarrow Bi(s). \quad (4)$$

The standard reduction potential of TeO_2 in equation (3) is 0.53 V, while the standard reduction potential of the Bi ions in equation (4) is 0.308 V [13]. When these two materials competitively undergo a reduction reaction, the standard reduction potential of TeO_2 is greater; this makes reduction easier as receiving an electron becomes easier. As a result, relatively more Te than Bi is deposited when EG is not added.

Table 1 shows the change of the Bi–Te composition and electrical resistivity according to the increase of EG content. When EG was not added, the atomic composition ratio of Bi to Te in the deposited alloy film was 1.66:3.34, where the content of Te was greater. On the other hand, when the EG addition rate was 40%v/v, the atomic composition ratio of Bi to Te was 2.56:2.44, where the content of Bi was greater. The criterion that separates the n-type and p-type is an atomic composition ratio of Bi:Te = 2:3, which corresponds to a Bi content of 40% when converted to a percentage. Fig. 7 shows the Bi content as a percentage according to the increase of EG content. As can be seen in the graph, the Bi content has a slope of 0.463 and shows a relatively linear increase. When EG was not added, it was observed that the deposited material, which was of n-type, changed to p-type, with the content reaching approximately 20%v/v. Without addition of EG, the Seebeck coefficient was a negative value (−76.3 μV/K). In contrast, in the case of EG content of 30%v/v, the Seebeck coefficient was a positive value (65.1 μV/K).

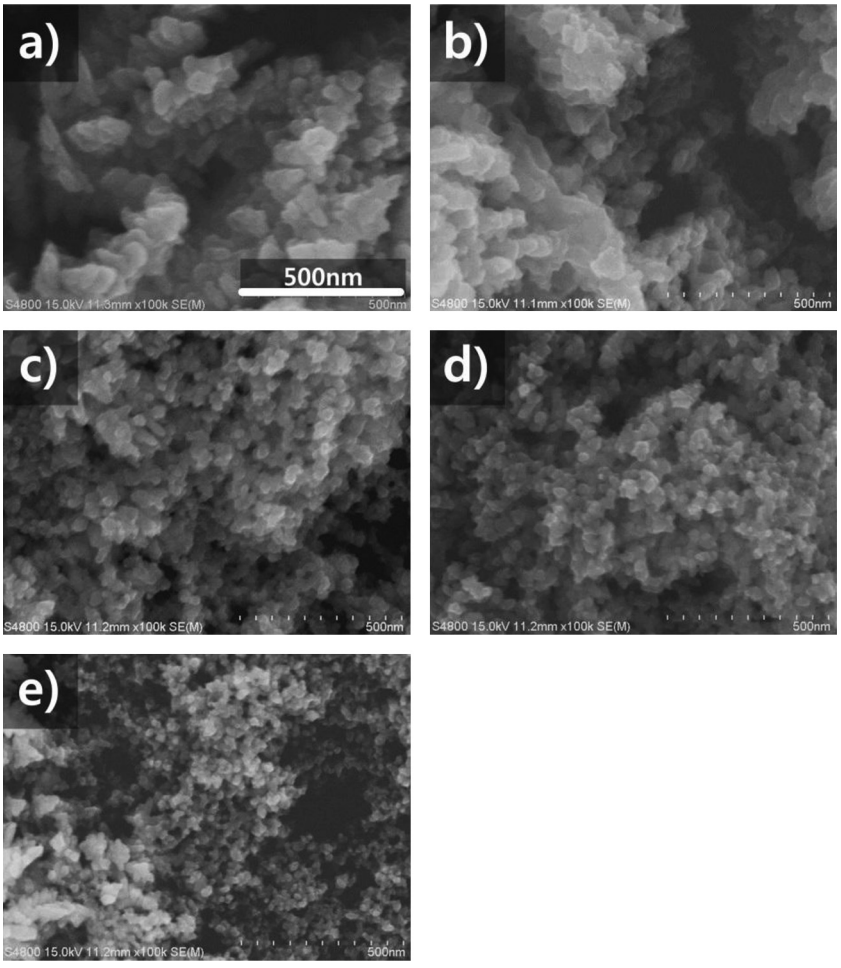

Fig. 6. SEM images of Bi–Te films deposited from various concentrations of ethylene glycol: (a) 0%v/v; (b) 10%v/v; (c) 20%v/v; (d) 30%v/v; (e) 40%v/v. The size scales are same.

Table 1
Atomic composition ratios and electrical resistivities of Bi–Te films deposited from various concentrations of ethylene glycol in the electrolyte.

Concentration of ethylene glycol (%v/v)	0	10	20	30	40
Atomic composition ratio (Bi:Te)	1.66: 3.34	1.84: 3.16	2.06: 2.94	2.36: 2.64	2.56: 2.44
Electrical resistivity (μΩ·m)	0.95	0.28	1.11	2.21	2.18

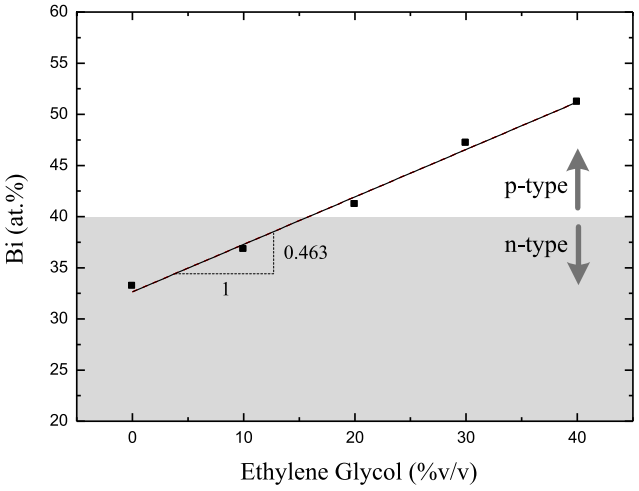

Fig. 7. Atomic percent of Bi in the deposited Bi–Te films by varying the concentration of ethylene glycol.

The above result can be attributed to two factors. First, it may be a result of the mass transfer change due to the increase in viscosity of the electrodeposition solution according to the addition of EG. While the viscosity of ethylene glycol is 1.61×10^{-2} N S/m^2, the viscosity of deionized water is 1.002×10^{-3} N S/m^2. Thus, the viscosity of EG is approximately 16 times greater than that of deionized water. This increase in viscosity affects the movement of the Bi ions and TeO_2. On the other hand, the atomic mass of the Bi ion is 208.08 u, while that of TeO_2 is 159.6 u. The diffusion velocity of materials within the solution is affected by the mass of the diffusion material [15]. The effect of viscosity is relatively greater with a smaller mass of diffusion material. Therefore, as the viscosity increases, the diffusion rate of TeO_2 with relatively smaller atomic mass becomes slower than that of Bi ions, resulting in a reduction of the amount of Te deposited.

Second, the result may be due to the limitation brought about by the mass transfer of TeO_2 due to the polarity of the EG molecule. EG has a chemical formula of $C_2H_6O_2$, with each ending having a polar OH. This OH has a bond angle of 104.5° and reacts with the oxygen atom of polar H_2O, forming a covalent bond and having the property of absorbing water [16]. The TeO_2 has a bond angle of 140° and

Table 2
Seebeck voltages, internal resistances, and output powers of the fabricated TEGs by varying the number of thermocouples.

Number of thermocouples	1	2	3	5
Seebeck voltage (mV)	1.40 ± 0.15	2.75 ± 0.12	4.22 ± 0.17	7.01 ± 0.29
Internal resistance (Ω)	20.4 ± 1.2	39.7 ± 1.4	60.2 ± 1.1	100.0 ± 1.9
Output power (nW)	24.36 ± 6.28	47.92 ± 5.85	74.21 ± 7.31	124.95 ± 10.85

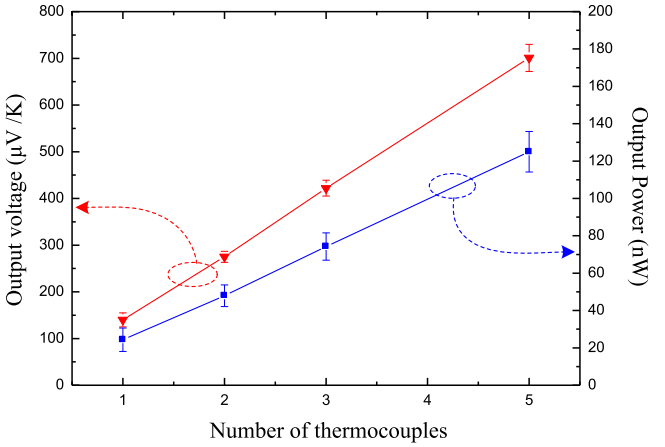

Fig. 8. Output voltage and output power of the fabricated TEGs by varying the number of thermocouples.

polarity, thus being able to form a covalent bond with EG due to the oxygen atoms at each end. Therefore, when the EG content increases, more TeO_2 bonds with EG, resulting in a reduction of the amount of Te deposited.

Through the results of this study, it was confirmed that controlling the Bi–Te composition ratio is possible by controlling the EG content included in the Bi–Te electrodeposition solution. Diffusion of the solution occurs during the pulse off-time, advantageously allowing electrodeposition with a uniform composition [12].

3.2. Bi–Te thermoelectric generator

The Seebeck voltages, internal resistances, and maximum output powers obtained from the fabricated TEGs are listed in Table 2. Three devices were selected for each thermocouple number and each device was measured five times. The Seebeck voltage measured from a fabricated thermocouple was 1.40 ± 0.15 mV. Considering the temperature difference (10 °C) applied during measurement of the thermocouple, the measured voltage is similar to the difference (141.4 μV/K) in the Seebeck coefficients of the two thermoelectric films (0%v/v EG: −76.3 μV/K, 30%v/v EG: 65.1 μV/K). As shown in Fig. 8, the Seebeck voltages linearly increased according to the number of thermocouples. The output powers were obtained by plugging the measured Seebeck voltages and internal resistances into equation (2). The output power of a fabricated thermocouple was 24.36 ± 6.28 nW and the output powers linearly increased with the number of thermocouples, as shown in Fig. 8. It is expected that output power of 2.39 μW could be produced per square centimeter. In this study, the output power was not very high due to the high internal resistance. Generally, there is a high contact resistance between metal and a semiconductor because of the metal-semiconductor contact resistance effect. To increase the output power, it is thus necessary to reduce the contact resistance between the copper interconnects and thermoelectric columns. Because electrodeposited Bi–Te materials are brittle, it is difficult to fabricate flexible TEGs using them. As done in this study, however, Bi–Te thermoelectric materials can be formed in a micro-column shape and embedded in a thin polymer plate; the fabricated TEGs could thus be applied to flexible thermoelectric devices.

4. Conclusion

Bi–Te composition ratio has simply been controlled by the addition of EG in the Bi–Te co-electrodeposition solution. N-type

and p-type thermoelectric materials were selectively formed by the addition rate of EG. As the EG content was increased, the Bi content increased relatively in the deposited material while the Te content decreased. The Bi atom ratio in the deposited material according to the EG content had a slope of 0.463 (at.% of Bi/vol.% of EG) with a linear increasing trend. The deposited material, which was n-type when the EG content was below approximately 20%v/v, turned to p-type when the content exceeded this threshold. This demonstrates that adjusting the EG content in the electrodeposition solution afforded simple control over the Bi–Te composition ratio. Meanwhile, an increase in the EG content led to a decrease of the deposited material particle size. This change was due to an increase in the electrolytes from the addition of EG, which led to an increase in the overpotential during the electrodeposition process. To demonstrate the applicability of the developed thermoelectric materials, micro-TEGs were fabricated and their performances were evaluated. N-type thermoelectric columns were fabricated using a solution without EG, while p-type columns were fabricated via electrodeposition using an electrodeposition solution with 30% v/v EG. The Seebeck voltage measured from a fabricated TEG was 1.40 mV and the output power was 24.36 nW at a 10 °C temperature difference. The output powers of the fabricated devices increased almost linearly with the number of thermocouples.

Acknowledgment

This research was supported by the Pioneer Research Center Program through the National Research Foundation of Korea funded by the Ministry of Science, ICT and Future Planning (2010–0019313).

References

[1] V. Leonov, T. Torfs, P. Fiorini, C. van Hoof, Thermoelectric converters of human warmth for self-powered wireless sensor nodes, IEEE Sens. J. 7 (2007) 650–657.
[2] H. Zou, D.M. Rowe, G. Min, Preparation and characterization of *p*-type Sb_2Te_3 and *n*-type Bi_2Te_3 thin films grown by coevaporation, J. Vac. Sci. Technol. A 19 (2001) 899–903.
[3] D.-H. Kim, E. Byon, G.-H. Lee, S. Cho, Effect of deposition temperature on the structural and thermoelectric properties of bismuth telluride thin films grown by co-sputtering, Thin Solid Films 510 (2006) 148–153.
[4] R. Venkatasubramanian, T. Colpitts, E. Watko, M. Lamvik, N. El-Masry, MOCVD of Bi_2Te_3, Sb_2Te_3 and their superlattice structures for thin-film thermoelectric applications, J. Cryst. Growth 170 (1997) 817–821.
[5] M. Takahashi, Y. Muramatsu, T. Suzuki, S. Sato, M. Watanabe, K. Wakita, T. Uchida, Preparation of Bi_2Te_3 films by electrodeposition from solution containing Bi-ethylenediaminetetraacetic acid complex and TeO_2, J. Electrochem. Soc. 150 (2003) C169–C174.
[6] S. Li, M.S. Toprak, H.M.A. Soilman, J. Zhou, M. Muhammed, D. Platzek, E. Müller, Fabrication of nanostructured thermoelectric bismuth telluride thick films by electrochemical deposition, Chem. Mater. 18 (2006) 3627–3633.
[7] C.-L. Chen, Y.-Y. Chen, S.-J. Lin, J.C. Ho, P.-C. Lee, C.-D. Chen, S.R. Harutyunyan, Fabrication and characterization of electrodeposited bismuth telluride films and nanowires, J. Phys. Chem. 114 (2010) 3385–3389.
[8] H.P. Nguyen, M. Wu, J. Su, R.J.M. Vullers, P.M. Vereecken, J. Fransaer, Electrodeposition of bismuth telluride thermoelectric films from a nonaqueous electrolyte using ethylene glycol, Electrochim. Acta 68 (2012) 9–17.
[9] A.J. Naylor, E. Koukharenko, I.S. Nandhakumar, N.M. White, Surfactant-mediated electrodeposition of bismuth telluride films and its effect on microstructural properties, Langmuir 28 (2012) 8296–8299.
[10] W. Glatz, L. Durrer, E. Schwyter, C.r Hierold, Novel mixed method for the electrochemical deposition of thick layers of $Bi_{2+x}Te_{3-x}$ with controlled stoichiometry, Electrochim. Acta 54 (2008) 755–762.
[11] W. Glatz, S. Muntwyler, C. Hierold, Optimization and fabrication of thick flexible polymer based micro thermoelectric generator, Sens. Actuat. A 132 (2006) 337–345.
[12] M.S. Chandrasekar, M. Pushpavanam, Pulse and pulse reverse plating-conceptual, advantages and applications, Electrochim. Acta 53 (2008) 3313–3322.
[13] G. Milazzo, S. Caroli, R.D. Braun, Table of standard electrode potentials, J. Electrochem. Soc. 125 (1978) 261C.
[14] A.J. Bard, R. Parsons, J. Jordan, Standard Potentials in Aqueous Solutions, Marcel Dekker, New York, 1985.
[15] Mark F. Mathias, Thomas W. Chapman, The composition of electrodeposited Zinc-nickel alloy coatings, J. Electrochem. Soc. 134 (1987) 1408–1416.
[16] M.J. Kao, D.C. Tien, C.S. Jwo, T.T. Tsung, The study of hydrophilic characteristics of ethylene glycol, in: Journal of Physics: Conference Series, 7th International Symposium on Measurement Technology and Intelligent Instruments, 13, 2005, pp. 442–445.